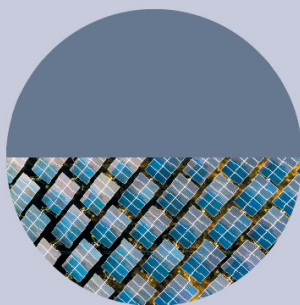


PAPER • OPEN ACCESS

Evaluation of topographic data sources for 2D flood modelling: case study of Kelani basin, Sri Lanka

To cite this article: A C A Suja and R L H L Rajapakse 2020 *IOP Conf. Ser.: Earth Environ. Sci.* **612** 012043

View the [article online](#) for updates and enhancements.



ENVIRONMENTAL RESEARCH
INFRASTRUCTURE AND SUSTAINABILITY™

No publication charges until 2021. Submit your research iopscience.org/eris

Editor-in-Chief

Arpad Horvath, University of California, Berkeley, USA

Evaluation of topographic data sources for 2D flood modelling: case study of Kelani basin, Sri Lanka

A C A Suja^{1,2,3} and R L H L Rajapakse¹

¹ Department of Civil Engineering, University of Moratuwa, Sri Lanka

² Department of Civil Engineering, South Eastern University of Sri Lanka, Sri Lanka

³ E-mail: acasuja@seu.ac.lk

Abstract. Frequent flooding in Sri Lanka underscores the necessity of flood modelling as inundation extent and flood depth can easily be identified for implementing flood control measures. Accuracy of flood modelling is primarily influenced by topographic data sources and their resolution. Due to the lack of Light Detection and Ranging (LiDAR) data source in most regions of Sri Lanka, alternative topographic data sources need to be assessed. This paper investigates the accuracy of 2D flood model results in terms of flood depth and inundation extent developed based on open source topographic data sources, namely Shuttle Radar Topography Mission (SRTM) and Advanced Spaceborne Thermal Emission (ASTER) with 30 and 90 m resolutions. This study was carried out at the downstream of Kelani river basin as it is prone to frequent flooding. The 1 m resolution LiDAR data were used as the reference data to assess the accuracy of aforesaid data sources, and were resampled to 30 and 90 m to investigate the effect of resolution with SRTM and ASTER data sources. The results show that reduction in the resolution of LiDAR data source does not significantly affect the model accuracy as even 90 m resolution LiDAR data source produced higher accurate results (flood depth, root mean square error of 0.95 m; inundation extent, F-statistic of 70.21%) than the 30 m resolution SRTM and ASTER data sources.

1. Introduction

Floods are identified as one of the most common and destructive natural hazards in several parts of the world [1]. Floods cause several impacts on the society, namely economical losses, environmental and social problems and human casualties [2]. In Sri Lanka, floods occur due to extreme rainfall during the two monsoons, namely Northeast (November-February) and Southwest (May-September), which are caused by the development of extreme low pressure in the Bay of Bengal. The both monsoons are caused by differing temperature trends over the land and ocean. Among all the river basins, Kelani, Kalu, Gin, Nilwala and Mahaweli are susceptible to frequent flooding affecting an approximate area of 250 km² and involving more than one million people [3]. Much more attention needs to be given on flood impacts of Kelani river as part of the capital of Sri Lanka lie on the lower floodplain of the river and those areas are prone to flooding due to the overflow of Kelani river during Southwest monsoon. Flood impacts caused due to the overflow of Kelani river in the recent past have underscored the necessity of developing reliable flood models as it is the preferred approach to identify flood depth and inundation extent of the flood [4]. Thus, it is useful to make awareness amongst people who are living in the floodplain and to implement rescue and relief operations during the flooding [5] and avoid future constructions on the flood risk areas [6].



Reliability of flood model results depends on the accuracy of flood modelling [5] and topographic data sources and their resolution play an important role in determining the accuracy of flood modelling [5, 7]. Topography is represented in the form of a raster, which is commonly known as Digital Elevation Model (DEM). There are different methods available to develop DEMs, namely photogrammetric method, interferometry, Light Detection and Ranging (LiDAR) technology, aerial photography and topographic surveys [8, 9]. Among all these methods, LiDAR technology serves as an accurate technique to produce highly accurate topographic datasets [10-12]. However, many locations in Sri Lanka and around the world do not have LiDAR data due to the cost of data acquisition and time constraints [12, 13].

In Sri Lanka, LiDAR survey (1 m resolution) was carried out by Survey Department of Sri Lanka in collaboration with Japan International Cooperation Agency (JICA) in 2016, covering small regions of the country as depicted in Figure 1. The distinct zones A, B, C, and D marked on Figure 1 denote the frequent flood prone basins in Sri Lanka, namely Kelani, Kalu, Gin and Nilwala, respectively. It is clearly shown that some reaches of Kelani and Kalu basins are covered with LiDAR data whereas Gin and Nilwala river basins have not been covered at all.

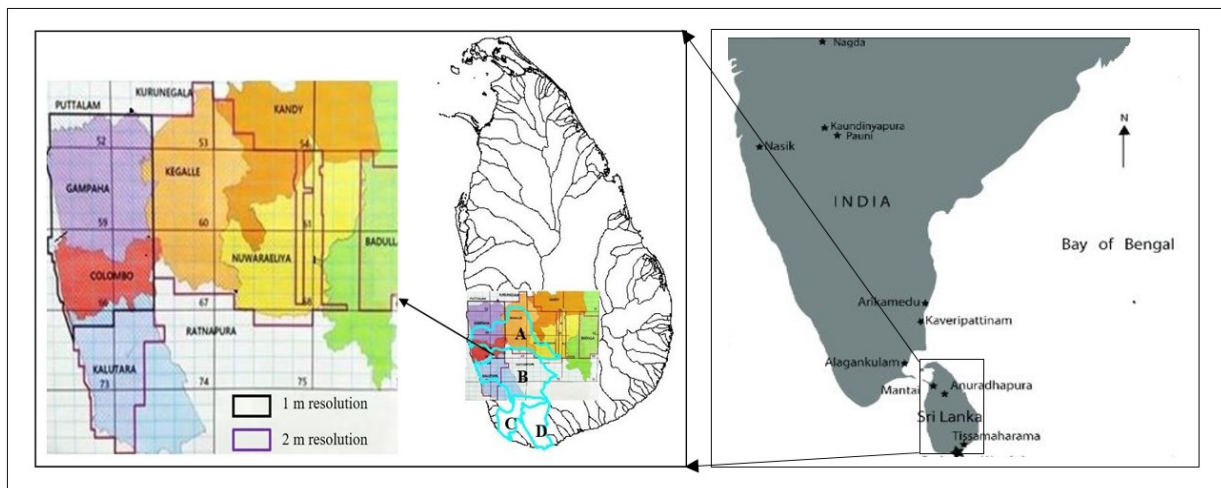


Figure 1. LiDAR data availability in Sri Lanka.

Most of the past studies were extensively carried out using one-dimensional (1D) modelling due to the computation simplicity and shorter computational time even though it has many shortcomings, namely incapability to represent the whole topography of river channel and floodplains, incapability to model lateral flow and less detailed between modelled cross-sections [7, 14]. These shortcomings of 1D models can be overcome by applying two-dimensional (2D) modelling and they are capable of modelling lateral flow movement explicitly with the continuous representation of topography [7, 15]. However, the main drawback of 2D models when compared with the 1D model is the substantial computational time required for the simulation [6].

Therefore, the primary objective of this study is to assess the accuracy of freely available topographical data sources in Sri Lanka, namely Shuttle Radar Topography Mission (SRTM) and Advanced Spaceborne Thermal Emission (ASTER) with 30 and 90 m resolutions for 2D flood modelling. The 1 m resolution LiDAR dataset was used as a reference dataset to assess the accuracy of aforesaid datasets and was resampled to 30 and 90 m to investigate the effect of the resolution against SRTM and ASTER datasets.

2. Materials and methods

2.1. Study area

Kelani basin is located between 6.78°N to 7.08°N latitudes and between 79.87°E to 80.72°E longitudes with a basin area of 2230 km². A downstream reach of about 25 km in length from Hanwella to Colombo covering an area of 250 km² was selected for this study as depicted in Figure 2. Extents of floodplain from left bank and right bank of the Kelani river was demarcated based on the past observed flood inundation extents corresponding to the flood events occurred in 2017 and 2018 since those flood events were considered as baseline data in this study.

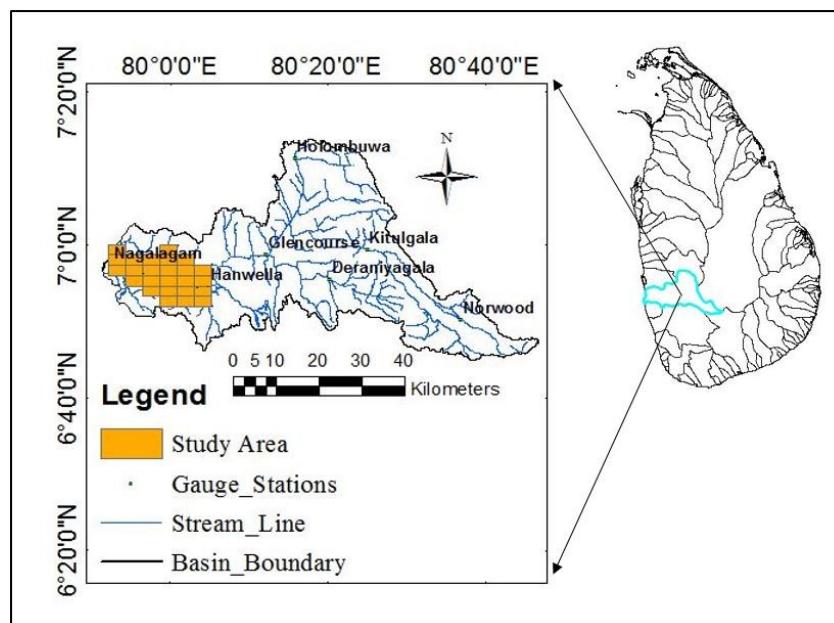


Figure 2. Study area covering downstream of Kelani basin from Hanwella to Colombo.

2.2. Topographic data sources

The 1 m high resolution LiDAR dataset which was produced by the Survey Department of Sri Lanka in collaboration with Japan International Cooperation Agency (JICA) in 2016 was used as reference dataset in the study.

SRTM is one of freely available DEMs, which was completed in 2000, and provides the first high resolution DEM data of near global scale [16]. The SRTM data were released publicly in 2003, for many parts of the world with 90 m resolution and 30 m resolution covering only the region of the United States and its territories. After the year of 2015, 30 m resolution datasets were also publicly distributed by the United States Geological Survey (USGS) along with the 90 m data [9]. For this study, 30 m resolution dataset was downloaded from the USGS website whereas 90 m resolution dataset was downloaded from CGIAR-CSI website.

The 1st version of the ASTER dataset, released in June 2009, was compiled from over 1.2 million scene-based DEMs covering land surface between 83° North and 83° South latitudes, involving 99% of Earth's landmass [9, 17]. The 2nd version of the ASTER dataset was released by the METI of Japan and NASA of United States in October 2011. For this study, the 30 m resolution dataset was downloaded from the USGS website.

The 1 m LiDAR dataset depicted in Figure 3 was used as reference dataset to assess the effect of different topographic data sources and their resolution on the accuracy of 2D flood modelling in terms of two model outputs, namely inundation extent and flood depth. In order to perform this task, six models were developed, i.e. two models with 30 m and 90 m resolutions from each dataset, namely LiDAR,

SRTM and ASTER as shown in Figure 4. The ArcGIS 10.3 (ESRI) was used to resample the 1 m resolution LiDAR dataset into 30 and 90 m resolution datasets, and 30 m resolution ASTER dataset into 90 m dataset using the nearest neighbour resampling method [9].

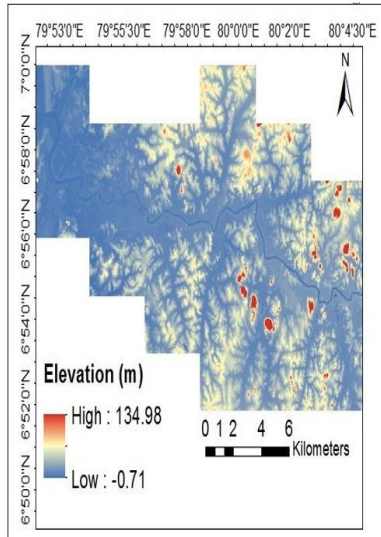


Figure 3. Reference data.

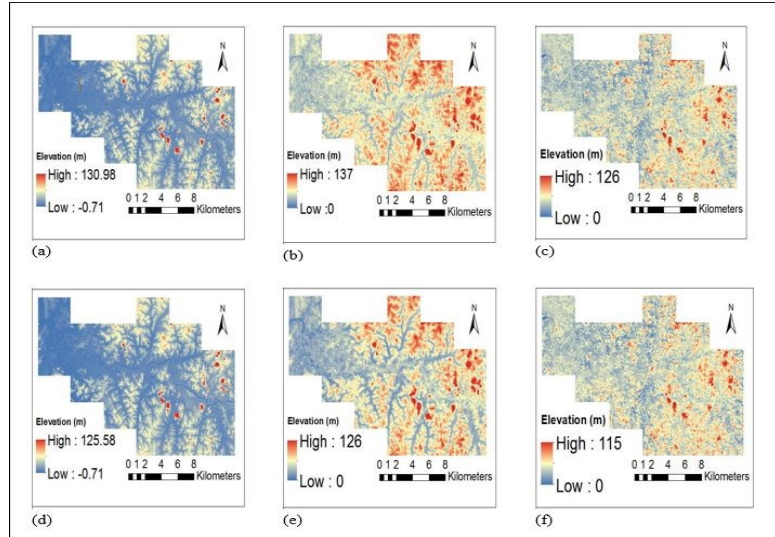


Figure 4. Datasets used in the study: (a) LiDAR 30 m; (b) SRTM 30 m; (c) ASTER 30 m; (d) LiDAR 90 m; (e) SRTM 90 m; (f) ASTER 90 m.

2.3. Hydraulic modelling

2.3.1. 2D flood model. The Nays2D Flood solver developed by the International River Interface Cooperative (iRIC) (Hokkaido University, Japan) was used in this study. Nays2D Flood is an open-source software that solves shallow water computations using the finite difference scheme [18]. The set of continuity and momentum equations of 2D unsteady flow in the Cartesian coordinate system are given in equations (1-3);

Continuity equation:

$$\frac{\partial h}{\partial t} + \frac{\partial(hu)}{\partial x} + \frac{\partial(hv)}{\partial y} = 0 \quad (1)$$

Momentum equations:

$$\frac{\partial hu}{\partial t} + \frac{\partial(hu^2)}{\partial x} + \frac{\partial(huv)}{\partial y} = -gh \frac{\partial H}{\partial x} - \frac{\tau_{bx}}{\rho} + \frac{\partial}{\partial x} \left(V \frac{\partial(hu)}{\partial x} \right) + \frac{\partial}{\partial y} \left(V \frac{\partial(hu)}{\partial y} \right) \quad (2)$$

$$\frac{\partial hv}{\partial t} + \frac{\partial(huv)}{\partial x} + \frac{\partial(hv^2)}{\partial y} = -gh \frac{\partial H}{\partial y} - \frac{\tau_{by}}{\rho} + \frac{\partial}{\partial x} \left(V \frac{\partial(hv)}{\partial x} \right) + \frac{\partial}{\partial y} \left(V \frac{\partial(hv)}{\partial y} \right) \quad (3)$$

where h = water depth; u, v = depth-averaged velocity components; τ_{bx} = riverbed shear stress in the x -direction; τ_{by} = riverbed shear stress in the y direction; ρ = the water density; H = stage height ($H = h + z_b$); z_b = bed elevation; V = eddy viscosity; t = time; and x, y = spatial coordinates in the Cartesian system. Bed shear stress components are given in equations (4-6);

$$\tau_{bx} = \rho C_f u \sqrt{u^2 + v^2} \quad (4)$$

$$\tau_{by} = \rho C_f v \sqrt{u^2 + v^2} \quad (5)$$

$$v = \frac{k}{6} uh \quad (6)$$

where C_f = riverbed friction coefficient; k = Karman constant; and u = shear velocity.

The above equations which are in the Cartesian coordinate system were transformed into the moving boundary-fitted coordinate system using the Jacobian chain rules. The high-order Godunov scheme known as Cubic Interpolation Pseudoparticle (CIP) method was used for application of the equations of water flow. This method interpolated physical values between grid points at the previous time step by using cubic equation under the assumption that spatial gradients of those physical values were also transported by similar convective equations. Information on a small number of adjacent cells is enough for this approach to compute precise profiles of convectional variables [19, 20].

2.3.2. Model configuration. The flow hydrograph (peak discharge $1449 \text{ m}^3 \text{ s}^{-1}$) observed at Hanwella hydrometric station during the flood event occurred in 2017 was used as upstream boundary condition whereas tidal variation was used in the downstream boundary condition as river mouth is connected to the sea. The calculation time step was set for 0.2 sec for 1 m resolution, 0.8 sec for 30 m resolution and 1.2 sec for 90 m resolution datasets which satisfied Courant-Friedrichs-Lewy (CFL) condition. Model results were exported to ArcGIS (ESRI) to develop inundation maps and carry out further analyses of model accuracy.

As the laser and radar waves used in the development of LiDAR, SRTM and ASTER datasets are not capable of penetrating the water surface and capturing the elevation of river cross-sections, all DEMs used in the study were incorporated with surveyed river cross-section data, which were carried out by Sri Lanka Navy using bathymetry boat survey in 2017, at about the interval of 100 m between each cross-section.

2.4. Evaluation of model calibration and validation

Water levels observed at an hourly time step in Ambatale peripheral hydrometric station in 2017 (23rd May to 28th May) and 2018 (19th May to 24th May) flood events were used for calibration and validation, respectively. Manning's roughness coefficients of channel and floodplain [4, 7] were used as model parameters to calibrate the model. The land cover map developed using ArcGIS (ESRI) software was used to assign the Manning's roughness coefficients for different land use types. The goodness of fit between simulated and observed water levels was numerically analysed using objective functions, namely Nash-Sutcliffe Efficiency (NSE) [21], Percentage Bias (PBIAS) [22] and Mean Relative Absolute Error (MRAE) [23], and those are given in equations (7-9);

$$\text{NSE} = 1 - \frac{\sum_{i=1}^n (O_i - S_i)^2}{\sum_{i=1}^n (O_i - \bar{O})^2} \quad (7)$$

$$\text{PBIAS} = \frac{\sum_{i=1}^n (O_i - S_i) \times 100}{\sum_{i=1}^n O_i} \quad (8)$$

$$\text{MRAE} = \frac{1}{n} \sum_{i=1}^n \frac{|S_i - O_i|}{O_i} \quad (9)$$

where O_i and S_i are the observed and simulated water levels in i^{th} hour; \bar{O} is the mean of observed water level; n is the total number of hours. Higher rating of model performance is attained when value of NSE approaches to 'one' whereas values of PBIAS and MRAE approach to 'zero'.

2.5. Evaluation of model accuracy

Accuracy of model results developed by different topographic data sources and their resolutions was assessed in terms of two hydraulic contexts, namely flood depth and inundation extent. For flood depth analysis, flood depth corresponding to each node, developed by each model was assessed with respect to the reference model using Root Mean Square Error (RMSE) which is given in equation (10);

$$\text{RMSE} = \left[\frac{1}{n} \sum_{i=1}^n (D_{iRef} - D_{iDEM})^2 \right]^{\frac{1}{2}} \quad (10)$$

where D_{iRef} and D_{iDEM} are depth simulated by reference DEM and other DEMs in i^{th} node; n is the total number of nodes analysed. The quantitative comparison of inundation extents developed by different models was assessed using F-statistic (measure of fit) (F), which is given in equation (11);

$$F (\%) = \frac{A_1 \cap A_2}{A_1 \cup A_2} \times 100 \quad (11)$$

where A_1 and A_2 are simulated and observed (i.e. simulated by the reference model) inundation areas; \cap and \cup are the 'Intersection' and 'Union' operations performed in ArcGIS, respectively. The highest possible value of F is 100%, which is attained when the two inundation areas are completely overlapped.

3. Results and discussion

3.1. Summary of model calibration and validation

Model performance was assessed at the calibration and validation in terms of objective functions and those values are tabulated in Table 1. The values of the objective function show good agreement between simulated and observed water levels as they are within the accepted ranges specified in the literature [24, 25]. Manning's roughness coefficients for the different land use assigned during calibration and validation are presented in Table 2.

Table 1. Values of objective functions.

Objective functions	Calibration	Validation	Accepted criteria
PBIAS	5.61%	8.56%	<25%
Nash-Sutcliffe	0.80	0.55	>0.5
MRAE	0.11	0.13	<0.25

Table 2. Manning's roughness coefficients.

Land use	Value
Agriculture	0.070
Marsh	0.040
Paddy	0.045
Roads	0.030
Residence	0.075
River channel	0.035

3.2. Effect of topographic data sources and their resolution on model accuracy

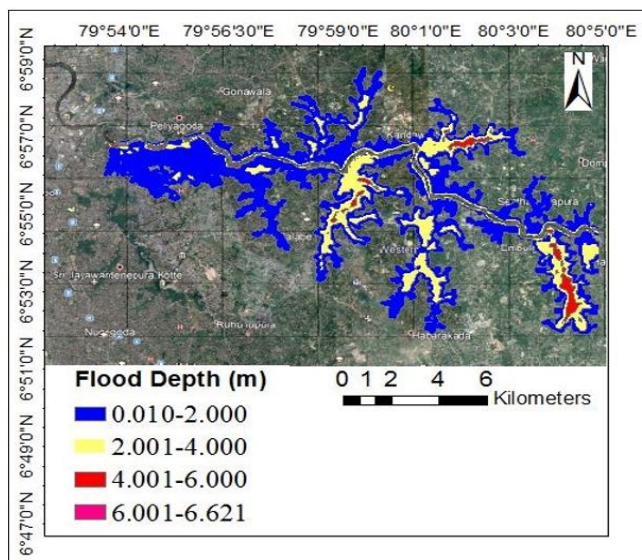
3.2.1. Flood depth. The flood depth corresponding to each node, developed by each model was exported to ArcGIS and 'Attribute and table operations' were performed to evaluate the accuracy on flood depth simulated by different datasets with respect to reference dataset in terms of RMSE and those values are tabulated in Table 3.

Among all six datasets, resampled LiDAR datasets (30 m and 90 m resolution) performed better than the SRTM and ASTER datasets with 30 m and 90 m resolutions (Table 3). Moreover, it is important to note that even the 90 m LiDAR dataset shows higher accuracy (RMSE = 0.95 m) than the 30 m resolution SRTM and ASTER datasets (RMSE values are 1.49 m and 1.54 m, respectively). This result suggests a decrease in the resolution of LiDAR from 1 m to 90 m does not significantly affect the model accuracy in terms of flood depth compared to SRTM and ASTER datasets. However, when considering SRTM and ASTER datasets, reduction in resolution from 30 m to 90 m leads to an increase in RMSE values which ultimately leads to a significant reduction in accuracy. Another notable result is that RMSE increases when resolution decreases from 30 m to 90 m for all datasets, namely LiDAR, SRTM and ASTER. Furthermore, 90 m resolution ASTER dataset shows the least accuracy among all datasets with RMSE value of 1.63 m.

Table 3. RMSE values of different datasets.

Dataset	RMSE (m)
LiDAR - 30 m	0.69
LiDAR - 90 m	0.95
SRTM - 30 m	1.49
SRTM - 90 m	1.63
ASTER - 30 m	1.54
ASTER - 90 m	1.63

3.2.2. *Inundation extent.* Inundation extent developed by reference model and other six models were exported to ArcGIS to produce inundation maps with different depth classification as depicted in Figures 5 and 6, respectively. Moreover, overlay operations, namely ‘Intersect’ and ‘Union’ were performed on inundation extents developed by each model with respect to reference model in order to calculate the F-statistic (measure of fit) of inundation extents, and those values are tabulated in Table 4.

**Figure 5.** Inundation extent map of reference model with different depth classifications.**Table 4.** F-statistic values.

Dataset	F (%)
LiDAR - 30 m	88.12
LiDAR - 90 m	70.21
SRTM - 30 m	62.13
SRTM - 90 m	58.47
ASTER - 30 m	40.54
ASTER - 90 m	37.83

Among all six models developed, 30 m resolution LiDAR model shows highest overlapping with the reference model with an F value of 88.12% whilst 90 m resolution LiDAR model shows an F value of 70.21%, where both values are higher than the values produced by SRTM and ASTER models with 30 m and 90 m resolutions. This result implies that reduction in the resolution of LiDAR dataset from 1 m to 90 m does not significantly affect the model accuracy in terms of inundation extent compared to SRTM and ASTER datasets. Another important result is to highlight that even 90 m resolution SRTM dataset show an F value of 58.47%, which is higher than the values produced by the ASTER 30 m model. Furthermore, 90 m resolution ASTER model shows the least accuracy among all models with an F value of 37.83%.

The findings of this study agree with some previous studies to a large extent. For instance, in a study carried out in Johor, Malaysia [10] to assess the different DEMs (LiDAR- 1 m, 20 m, 30 m and 90 m; SRTM- 90 m; ASTER- 30 m; contour maps - 20 m) on 1D hydraulic modelling, the results had indicated that even resampled 90 m resolution LiDAR dataset showed higher accuracy than all other datasets used.

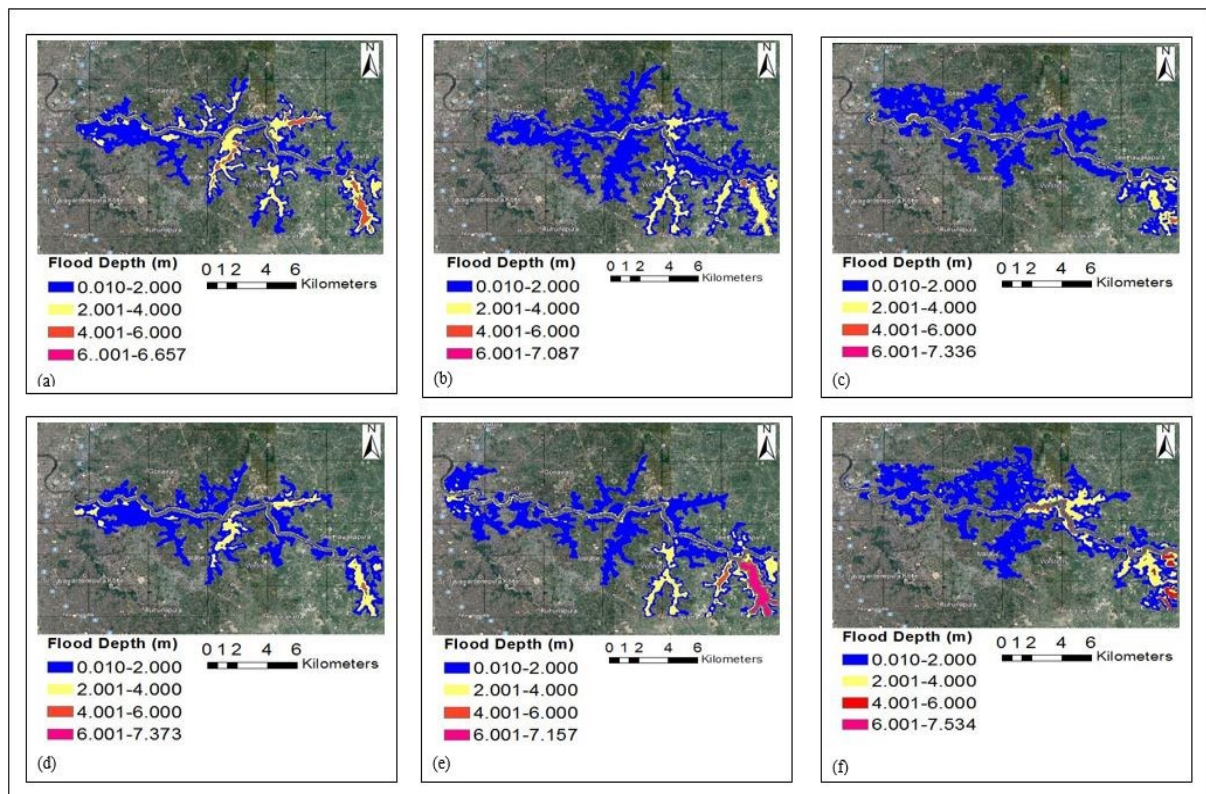


Figure 6. Inundation extent maps of all six models with different depth classifications: (a) LiDAR 30 m; (b) SRTM 30 m; (c) ASTER 30 m; (d) LiDAR 90 m; (e) SRTM 90 m; (f) ASTER 90 m.

4. Conclusions and recommendations

This study primarily assessed how different topographic data sources and their resolutions affect the accuracy of 2D flood modelling. This study was carried out at the downstream of Kelani basin, Sri Lanka where a 2D model was performed using Nays2D Flood solver. Six different datasets with resolutions of 30 m and 90 m derived from LiDAR, SRTM and ASTER were compared with a 1 m high resolution LiDAR dataset as reference, in terms of flood depth and inundation extent. Among all the datasets used in the study, 30 m resolution LiDAR dataset produced higher accurate results in terms of both hydraulic contexts, namely flood depth and inundation extents. Moreover, even 90 m resolution LiDAR dataset also showed higher accuracy than the SRTM and ASTER datasets with 30 m and 90 m resolutions.

In contrast, resolution variation from 30 m to 90 m does affect the model results of SRTM and ASTER datasets in terms of flood depth and inundation extents (Tables 3 and 4). Apart from the LiDAR dataset, 30 m resolution SRTM dataset performed better than other three datasets, namely 90 m resolution SRTM, 30 m resolution ASTER and 90 m resolution ASTER. Another notable result is the model developed from 90 m resolution ASTER dataset showed the least accuracy than all models in terms of flood depth and inundation extent. The findings of the present study are precisely limited to the specific site. However, this methodology can be applied to similar basins in Sri Lanka to verify the robustness of the results obtained.

References

- [1] Oganian J L, Puno G R, Alivio M B T and Taylaran J M G 2019 *Global J. Environ. Sci. Manag.* **5**(1) 95-106
- [2] Hartnett M and Nash S 2017 High-resolution flood modeling of urban areas using MSN Flood *Water Sci. Eng.* **10**(3) 175-83

- [3] Gunasekara I P A 2008 Flood hazard mapping in lower reach of Kelani basin *Engin. J. Instit. Engin., Sri Lanka* **45**(2) 149-54
- [4] Pinos J, Timbe L and Timbe E 2019 Evaluation of 1D hydraulic models for the simulation of mountain fluvial floods: a case study of the Santa Bárbara River in Ecuador *Water Pract. Technol.* **14**(2) 341–54
- [5] Cook A and Merwade V 2009 Effect of topographic data, geometric configuration and modeling approach on flood inundation mapping *J. Hydrol.* **377** 131–42
- [6] Bates P D and De Roo A P J 2000 A simple raster based model for flood inundation simulation *J. Hydrol.* **236**(1–2) 54–77
- [7] Pinos J and Timbe L 2019 Performance assessment of two-dimensional hydraulic models for generation of flood inundation maps in mountain river basins *Water Sci. Eng.* **12**(1) 11-8
- [8] Ali A, Solomatine D P and Di Baldassarre G 2015 *Hydrol. Earth Syst. Sci.* **19**(1) 631–43
- [9] Mukherjee S, Joshi P K, Mukherjee S and Ghosh A 2013 *Int. J. Appl. Earth. Obs.* **21**(1) 205–17
- [10] Charlton M E, Large A R G and Fuller I C 2003 *Earth Surf. Process. Landf.* **28**(3) 299–306
- [11] Hodgson M E, Jensen J R, Schmidt L, Schill S and Davis B 2003 *Remote. Sens. Environ.* **84** 295–308
- [12] Sanders B F 2007 *Adv. Water. Resour.* **30**(8) 1831–43
- [13] Pham H T, Marshall L, Johnson F and Sharma A 2018 *Remote Sens. Environ.* **210** 229–41
- [14] Horritt M S and Bates P D 2001 *Hydrol. Process.* **15**(5) 825–42
- [15] Kourgialas N N and Karatzas G P 2013 *Hydrol. Process.* **27**(4) 515–31
- [16] Farr T and Kobrick M 2001 The shuttle radar topography mission *Amer. Geophys. Union EOS* **81** 583–5
- [17] Chaieb A, Rebai N and Bouaziz S 2016 *J. Geogr. Inf. Syst.* **8** 57–64
- [18] Nelson et al. 2016 The international river interface cooperative: Public domain flow and morphodynamics software for education and applications *Adv. Water. Resour.* **93** 62-74
- [19] Jang C L and Shimizu Y 2005 Numerical simulation of relatively wide, shallow channels with erodible banks. *J. Hydraul. Eng.* **131**(7) 565–575
- [20] Wongs S 2014 Simulation of Thailand Flood 2011 *Int. J. Eng. Technol.* **6**(6) 452–8
- [21] Nash J E and Sutcliffe J 1970 River flow forecasting through conceptual models Part I-A discussion of principles *J. Hydrol.* **10**(3) 282–90
- [22] Gupta H V, Sorooshian S and Yapo P O 1999 Status of automatic calibration for hydrologic models: comparison with multilevel expert calibration *J. Hydrol. Eng.* **4**(2) 135–43
- [23] World Meteorological Organization 1975 *Inter-comparison of conceptual models used in operational hydrological forecasting* (Geneva Switzerland: Operational hydrology report no.7/WMO- No 429)
- [24] Moriasi D N, Arnold J G, Lewis M W V, Bingner R L, Harmel R D and Veith T L 2007 *Amer. Soc. Agricul. Biol. Eng.* **50**(3) 885-900
- [25] Waseem M, Mani N, Andiego G and Usman M 2017 A review of criteria of fit for hydrological models *Int. Res. J. Eng. Technol.* **4**(11) 1765-72